CHAPTER XV

NEUTRINO AND MUON PHYSICS IN THE COLLIDER MODE OF FUTURE ACCELERATORS

A. De Rújula and R. Rückl

NEUTRINO AND MUON PHYSICS IN THE COLLIDER MODE OF FUTURE ACCELERATORS*)

A. De Rújula and R. Rückl
CERN, Geneva, Switzerland

ABSTRACT

Extracted beams and fixed target facilities at future colliders (the SSC and the LHC) may be (respectively) impaired by economic and "ecological" considerations. Neutrino and muon physics in the multi-TeV range would appear not to be an option for these machines. We partially reverse this conclusion by estimating the characteristics of the "prompt" ν_μ, ν_e, ν_τ and μ beams necessarily produced (for free) at the pp or $\bar{p}p$ intersections. The neutrino beams from a high luminosity (pp) collider are not much less intense than the neutrino beam from the collider's dump, but require no muon shielding. The muon beams from the same intersections are intense and energetic enough to study μp and μN interactions with considerable statistics and a Q^2-coverage well beyond the presently available one. The physics program allowed by these lepton beams is a strong advocate of machines with the highest possible luminosity: pp (not $\bar{p}p$) colliders.

I. INTRODUCTION

The interactions of muons and muon-neutrinos with nucleons have not been experimentally studied with beams of energy in the TeV range. The $\nu_e N$ interactions have been analysed in detail only at energies characteristic of β-decay. Not a single ν_τ has ever been seen to interact in a detector. These are sufficient reasons to justify a ν_e, ν_μ, ν_τ "program" at any future high energy facility, but one can say even more.

Much of the interest of ν_μ- and μ-scattering physics resides in the study of the deep inelastic nucleon structure functions $F_i(x,Q^2)$. Their measurements in light nuclei (H, D) are still statistically limited. In heavier targets (such as C and Fe) errors in F_2 are dominated by systematics and errors in xF_3^ν are both statistical and systematic. In neutrino experiments the systematic errors are dominated by the imprecision of hadron calorimetry, and would decrease with energy as $E^{-\frac{1}{2}}$. Errors in the measurement of the Q^2-evolution of the non-singlet structure function xF_3 jeopardize the cleanest tests of QCD. Very little is known about the ratio σ_L/σ_T. No experiments measuring $\mu \to \nu_\mu$ transitions have been performed. Besides testing conventional expectations, lepton scattering at higher energies could also reveal "nonstandard" physics: right-handed currents, new particle production, substructure of quarks and/or leptons, etc.[1]. Clearly much remains to be done in neutrino and muon physics.

Two high energy hadron colliders are now seriously discussed[2]. The American SSC would be a 20-on-20 TeV pp collider, for which we shall assume a luminosity $\mathcal{L} = 10^{33}$ cm^{-2} s^{-1}. The European LHC, to be placed atop LEP, may be a pp or $\bar{p}p$ machine. We shall assume the LHC beam energy to be 8 TeV, and the luminosity to be 10^{33} (10^{31}) cm^{-2} s^{-1} for the pp ($\bar{p}p$) options.

We allege in this paper that the production and prompt decay of charmed particles at the collider's intersection points is the source of energetic and highly collimated lepton beams, whose interest for physics is not negligible. The geometry and origin of these beams

*) A preliminary version was also included in the "Workshop on Fixed Target Physics at the SSC", Texas, 1984.

are shown in Fig. 1a,b, respectively. In Chapter II we derive the main characteristics (total flux and average energy) of the prompt lepton beams and compute the expected event rates at a hypothetical "standard" detector. In chapters III and IV we compare the neutrino and muon beams produced in the collider mode with the neutrino beams from a beam-dump, and with future ep facilities, respectively. Crucial to our considerations is an estimate of charm production cross sections at TeV energies. Our estimates are explained in detail in Appendix A. In Appendix B we predict the shapes of neutrino and muon beams as a function of energy and angle, and we estimate the evolution of the muon beam as it traverses an iron or soil shield.

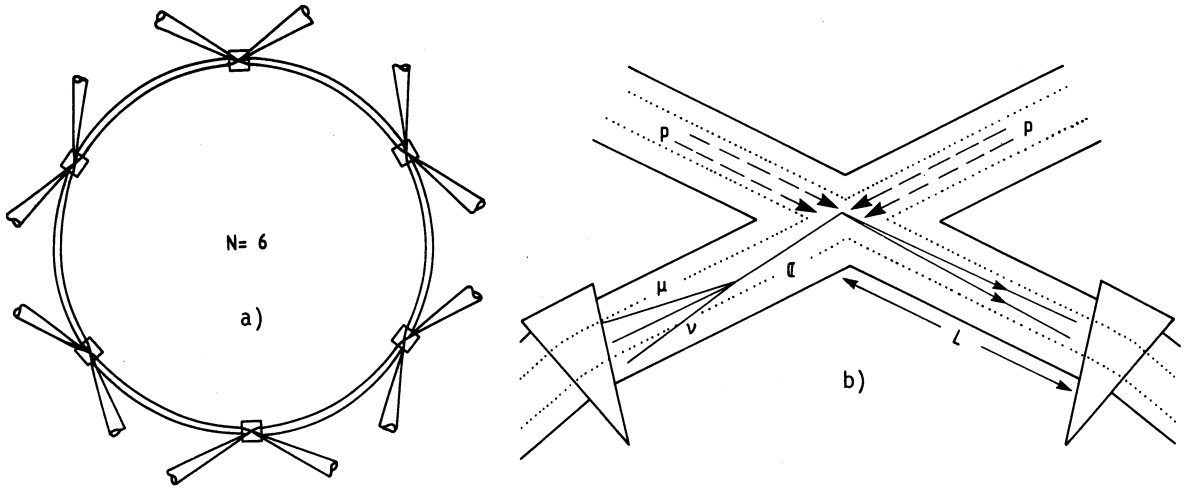

Fig. 1 a) The colliders' intersections (here 6) as a source of lepton beams. b) Charm (ℂ) origin of the lepton beams at a collision point.

II. PROMPT LEPTON BEAMS FROM THE INTERSECTION POINTS OF FUTURE pp ($p\bar{p}$) COLLIDERS

At the very high energies we are contemplating, the charm production cross-section σ_c is expected to be a good fraction of the total pp or $\bar{p}p$ cross-section σ_{tot}. We shall argue in detail in Appendix A, on the basis of an approximate universal scaling law of particle production, that $\sigma_c/\sigma_{tot} \geq 10\%$ is a very reasonable conservative estimate of charm production at these very high energies. Most of the produced charmed particles (all but the very high-p_T ones) fly and will decay within the straight sections of the beam pipe. To be convinced of this, assume charm to be produced with a Feynman-x distribution $(1-x)^n$, with n somewhere in between 0 and 5. The average energy of a charmed particle is $E_c = E_p/(n+2)$ and, hence, the typical decay length for $m_c \simeq 2$ GeV, $\tau_c \simeq 5 \times 10^{-13}$ secs is

$$d_c = \gamma c \tau_c \simeq (12\ \text{cm}) \left(E_p / 8\ \text{TeV} \right) \left(\frac{5}{n+2} \right) \qquad (1)$$

Approximately 10% of charmed particle decays contain an ($e\nu_e$) pair in the final state, another 10% contain a ($\mu\nu_\mu$) pair. The production fraction of each penetrating "prompt" lepton (μ, ν_e or ν_μ) is thus $0.1\ \sigma_c/\sigma_{tot} \gtrsim 0(1\%)$ of the total collision rate. It is on this fairly efficient way of making two lepton beams (a "leftwards" and a "rightwards" one) per collider intersection, that we shall capitalize.

The prompt lepton beams are naturally highly collimated. Let $\langle p_T \rangle$ be the average transverse momentum of the produced charmed particles. Their average production angle is $\theta_p \simeq \langle p_T/E_c \rangle \simeq (n+2)\langle p_T \rangle / E_p$. The average lepton angle θ_d in a typical "three-body" semi-leptonic charm decay is of order $(m_c - m_K)/(2E_c)$, with m_K the K or K^* mass. Hence, the average lepton to proton beam angle is of the order of

$$\theta \simeq \sqrt{\theta_p^2 + \theta_d^2} \simeq \sqrt{\langle p_T \rangle^2 + (m_c^2 - m_K^2)/4}\ \left(\frac{n+2}{E_p}\right) \tag{2}$$

For $\langle p_T \rangle$ = 1 GeV and n = 3

$$\theta \simeq (0.7\ \text{mrads})\,(8\ \text{TeV}/E_p) \tag{3}$$

The angular shape of the lepton beams is discussed in more detail in Appendix B.

The "contamination" in the prompt lepton beams from the decays of other heavy flavors, such as beauty, is quite negligible: the beauty production cross-section is only a small fraction of the charm production cross-section. More surprisingly, the contamination from π (or K) decay is also likely to be small at all lepton energies but the uninterestingly low ones. To be convinced of this, assume the leading-charged-pion x-distribution to be $(1-x)^{n_\pi}$, with n_π close to 4. The typical decay length of these pions is

$$d_\pi = \gamma c \tau_\pi \simeq \frac{E_p c}{(n_\pi+2) m_\pi} (2.6 \cdot 10^{-8}\ \text{secs}) \simeq 74\ \text{km} \left(\frac{6}{n_\pi+2}\right)\left(\frac{E_p}{8\ \text{TeV}}\right) \tag{4}$$

To estimate the contamination of leptons from π-decay in the "prompt" lepton beam, let L be the length of the colliding straight sections (after flying forward for L meters the pions will hit some material in the accelerator or the walls of the tunnel, and be lost as a source of hard leptons, see Fig. 1b). The ratio R of hard leptons from pions and charm is of the order

$$R = 10^{-3} \left(\frac{L}{74\ \text{m}}\right) \frac{\sigma_{tot}}{\sigma_c} \frac{1}{BR(c \to l\nu X)} \left(\frac{n_\pi+2}{6}\right) \tag{5}$$

For σ_c/σ_{tot} = 10% and even for a very long straight section with L = 74 m, R is of order 10%. It goes without saying that in the SSC, whose tunnel is not predetermined, theorists see no reason not to make a couple of diametrically opposed straight beam-tube sections be several kilometers long (a small fraction of the SSC's circumference!). These collision points would then be copious sources of (μ, ν_μ) from π decays and ν_e's from K decays.

We proceed to argue that no muon shielding preceding a neutrino experiment is necessary: all one needs is some 100 meters of soil to absorb the hadronic and electromagnetic showers from the primary collisions. Let N be the number of interaction regions in the collider. Consider a neutrino experiment placed somewhere along one of the 2N neutrino beams that the collider is tangentially producing for free. In a conventional neutrino experiment each machine burst produces zillions of muons that would completely blind the apparatus, unless efficiently absorbed and/or deflected. The muon and neutrino beams from a collider, on the other hand, are practically DC beams. Let the collider, for definiteness, be a pp machine with $\mathcal{L} = 10^{33}$ cm^{-2} s^{-1}. Assume σ_{tot} to be of order 150 mb[3]. The rate of pp collisions is thus 1.5×10^8/s. If (σ_c/σ_{tot}) BR$(c \to \mu\nu X)$ is 1%, the muon rate is 1.5×10^6/s. [For a 15(150) ns spacing between bunches this would correspond on average to one incoming muon every $\sim$ 40(4) beam crossings.] Surely a neutrino detector can stand this rate of single muons and could even be triggered by them, should one decide to sacrifice ν_e physics [neutrinos are unfortunately not "tagged" since the parent charmed particle momentum is not measurable]. The magnitude and shape of the incoming muon flux, as well as the $\mu \to \nu_\mu$ interactions and the high-Q^2 $\mu \to \mu$ interactions in the "neutrino" detector also offer interesting physics potential.

Let us now estimate the average ν and μ energies in the prompt beam, and the event rates to be expected in conventional-size detectors*). The main source of uncertainty in the shape of the fluxes is the longitudinal momentum distribution of the parent charmed particles. For D($\bar{D}$) production the least biased data are the ones from the LEBC-EHS collaboration[4], that "visually" measured charm production in pp collisions at $\sqrt{s}$ = 26 GeV. Within rather limited statistics, no significant difference in the x-distributions for D and $\bar{D}$ was observed, and the cross-section was found to be compatible with the form[4]

$$\frac{d\sigma}{dx\,dp_T^2} \propto (1-x)^n e^{-ap_T^2} \qquad \begin{cases} n = 1.8 \pm 0.8 \\ a = (1.1 \pm 0.3)\ \text{GeV}^{-2} \end{cases} \tag{6}$$

The smaller n is, the harder the x-distribution of the charmed particles, the "better" (more energetic and interactive) the ν and μ beams. In what follows we shall refer to a conservative choice n = 2 as our "optimistic" expectation for a D($\bar{D}$) x-distribution, and to n = 3 as the "pessimistic" choice. We shall assume F's to be produced with the same distribution as D's. The present experimental information on Λ_c production is even less satisfactory than the one on charmed mesons. Charmed baryons are candidates for a "leading particle effect" since they may contain two of the parent proton's valence quarks. The qualitative experimental indications are indeed that Λ_c's are harder than D's, with an exponent n compatible with 1, or even smaller, as suggested by certain theoretical models[5]. Our "optimistic"

*) The muon flux is degraded in energy and spread in angle as it crosses the hadron shield, an effect that we shall estimate in some detail in Appendix B. For an introductory estimate we shall assume the shield not to be much thicker than 25 kg/cm^2 (100 meters of soil or 30 meters of iron). In this case the muon flux is not seriously affected by its passage through the shield.

("pessimistic") assumption for the Λ_c x-distribution is n = 0.5 (n = 1). The lepton fluxes also depend on the assumed production cross-sections and leptonic branching ratios. Table 1 summarizes the "optimistic" (fairly conservative) and "pessimistic" inputs used in our extrapolations to higher energies.

Table 1

Parameters of our models of charm production

	$n(D,\bar{D},F)$	$n(\Lambda_c)$	$\frac{\sigma(\Lambda_c)}{\sigma(D+\bar{D})}$	$\frac{\sigma(F)}{\sigma(D+\bar{D})}$	$\frac{\sigma(F^+)}{\sigma(F^-)} = \frac{\sigma(D^+)}{\sigma(D^-)}$	$\frac{F \to \tau\nu_\tau}{F \to \text{all}}$
Optimistic	2	0.5	0.5	0.5	1	2%
Pessimistic	3	1	0.25	0.25	1	1%

In addition, we adopt the following semi-leptonic branching ratios for charmed particle decay[6]:

$$BR(D \to e\nu_e X) \sim 10\% \quad (D = D^+ + D^0) \tag{7a}$$

$$BR(\Lambda_c \to e\nu_e X) \sim 5\% \tag{7b}$$

$$BR(F \to e\nu_e X) \sim 15\% \tag{7c}$$

The D and Λ_c branching ratios are central experimental values, while the assumed BR(F) is the one expected from both "spectator" and "annihilation" decay mechanisms. To estimate $BR(F \to \tau\nu_\tau)$ we combine the measured lifetime with the theoretical expression for the purely leptonic decay[6]:

$$BR(F \to \tau\nu_\tau) = \Gamma(F \to \tau\nu_\tau) \cdot \tau_F \quad ; \quad \tau_F = \left(2.6 \,^{+1.8}_{-0.8}\right) 10^{-13}\ s$$

$$\Gamma(F \to \tau\nu_\tau) = \frac{G_F^2}{8\pi} f_F^2 \, m_F \, m_\tau^2 \left(1 - \frac{m_\tau^2}{m_F^2}\right)^2 \tag{8}$$

$$BR(F \to \tau\nu_\tau) = \left(1.7 \,^{+0.8}_{-0.5}\right) 10^{-2} \left(f_F / 200\ \text{MeV}\right)^2$$

The average $\nu(\ell^\pm)$ energy in a semi-leptonic "quasi-three body" decay, $c \to s\ell\nu$, of a high energy charmed particle is approximately $E_c/3$. The average energy of our lepton beams in $D,\Lambda_c,F \to \ell\nu X$ decays is thus $\langle E \rangle = E_p/(3n+6)$. In the decay of a fast F^+ into $\tau^+\nu_\tau$ the average $\nu_\tau(\tau)$ energies are $(1 \mp m_\tau^2/m_F^2)E_F/2$. In the subsequent $\tau^+ \to \bar{\nu}_\tau + \ldots$ decay the average neutrino energy is approximately $E_\tau/3$. Thus F^+'s produce ν_τ's ($\bar{\nu}_\tau$'s) with an average fraction 0.09 (0.3) of their energy. The expected average energies (in TeV) of the different lepton beam components are given in Table 2 for the choices E_p = 8, 20 TeV and for our two

models of charmed particle x-distributions. The quoted values are within 20% of the naïve estimates we just made, and come from more careful analytic and Monte Carlo calculations to be described in Appendix B.

Table 2

Average energies (in TeV) of the various components of the neutrino and muon beams

		$D \to \mu^+$ $\bar{D} \to \mu^-$	$D \to \nu_\mu, \nu_e$ $\bar{D} \to \bar{\nu}_\mu, \bar{\nu}_e$	$\Lambda_c \to \mu^+$	$\Lambda_c \to \nu_\mu, \nu_e$	$F^+ \to \nu_\tau$ $F^- \to \bar{\nu}_\tau$	$F^+ \to \tau^+ \to \bar{\nu}_\tau$ $F^- \to \tau^- \to \nu_\tau$
LHC	opt.	0.54	0.62	0.87	0.99	0.18	0.63
	pess.	0.44	0.49	0.72	0.82	0.14	0.50
SSC	opt.	1.36	1.55	2.18	2.47	0.45	1.58
	pess.	1.09	1.24	1.82	2.06	0.36	1.26

We proceed to estimate the total lepton fluxes and event rates. Let $\sigma_{tot}(\sigma_c)$ be the total (charm production) cross-section, let $\mathbb{C}(\ell)$ denote a particular charmed particle (lepton), and let $\mathcal{L}$ be the luminosity. The lepton flux is

$$\Phi_\ell = \frac{1}{2}\mathcal{L}\,\sigma_{tot}\left(\frac{\sigma_c}{\sigma_{tot}}\right)\left(\frac{\sigma(\mathbb{C})}{\sigma_c}\right) BR(\mathbb{C}\to\ell)\ \frac{\text{leptons}}{\text{second}} \tag{9}$$

Here, the factor $\frac{1}{2}$ reflects the fact that this is the flux in one of the two beams emitted by each interaction point. To estimate σ_{tot} we use the fit[3)]

$$\sigma_{tot} = \left[38.3 + 0.5\,\mathrm{Ln}^2(s/s_0)\right] \text{mb}\ ,\ s_0 = 116\ \text{GeV}^2 \tag{10}$$

which predicts σ_{tot} = 145(173) mb at LHC (SSC) energies. With our estimate $\sigma_c/\sigma_{tot} \gtrsim 10\%$ to be defended in Appendix A, we obtain

$$\Phi_\ell = \Phi_0\,\frac{\sigma(\mathbb{C})}{\sigma_c}\,BR(\mathbb{C}\to\ell) \tag{11a}$$

$$\Phi_0(\text{LHC}) = \frac{7.25\cdot 10^6}{\text{sec}}\left(\mathcal{L}/10^{33}\ \text{cm}^{-2}\,\text{sec}^{-1}\right) \tag{11b}$$

$$\Phi_0(\text{SSC}) = \frac{8.65\cdot 10^6}{\text{sec}}\left(\mathcal{L}/10^{33}\ \text{cm}^{-2}\,\text{sec}^{-1}\right) \tag{11c}$$

Let us now concentrate on the number of interactions produced by the neutrino beams. The

total (charged plus neutral-current) neutrino cross-sections per nucleon should at the relevant energies still be given by the approximate expression*)

$$\sigma_\nu\left(\frac{p+n}{2}\right) \equiv \sigma_{\nu N} \simeq 1.8\,\sigma_{\bar\nu N} \simeq 10^{-35}\,cm^2\left(\frac{E_\nu}{TeV}\right) \tag{12}$$

where we have used $\sin^2\theta_W \sim 0.21$. The number of neutrino interactions per centimeter per second in a detector whose transverse dimensions are larger than the beam width (recall the small divergence of the beam) is

$$\frac{dN}{dx\,dt} = \varrho N_A \int \phi_\nu(E_\nu)\,\sigma(E_\nu)\,dE_\nu$$
$$\simeq \varrho N_A\,(10^{-35}\,cm^2)\,\langle E_\nu\rangle\,\Phi_\nu \tag{13}$$

where ρ is the target density and N_A (nucleons/gr) is Avogadro's number. To be specific, consider an L = 25 meters-long detector of average density ρ = 5 gr/cm^3, exposed to the beam for a "working year" of Y = 10^7 seconds. The number of interactions in this detector, estimated from Eqs. 7 to 13 and Tables 1, 2 is given in Table 3. These estimates are obtained with the following $\sigma(\mathbb{C})/\sigma_c$ ratios, implied by Table 1:

$$\frac{\sigma(D,\bar D,\Lambda_c,F^+,F^-)}{\sigma_c} = \begin{cases} \left(\frac14,\frac14,\frac14,\frac18,\frac18\right) & \text{"optimistic"} \\ \left(\frac13,\frac13,\frac16,\frac{1}{12},\frac{1}{12}\right) & \text{"pessimistic"} \end{cases}$$

The $\tau^\pm$ leptons produced by charged current τ-neutrino interactions should at these high energies be visible with a detector of modest granularity. At the LHC, and in our "pessimistic" model, the average decay path of a τ^+ is 0.7 cm, if it is produced in the chain $F^- \to \bar\nu_\tau \to \tau^+$, and 2.5 cm if it comes from $F^+ \to \tau^+ \to \bar\nu_\tau \to \tau^+$. For a τ^- the decay lengths are 0.6 cm in the chain $F^+ \to \nu_\tau \to \tau^-$ and 2.0 cm for $F^- \to \tau^- \to \nu_\tau \to \tau^-$. At SSC energies, these numbers would increase by the machines' energy ratio $\sim$ 20/8.

We have mentioned that for a sufficiently short hadron shielding the prompt muon flux is practically unmodified. The shape of the $\mu^-(\mu^+)$ fluxes is similar to that of $\bar\nu_\mu(\nu_\mu)$. Thus, as in Table 3, we can easily estimate the number of $\mu^- \to \nu_\mu$ or $\mu^+ \to \bar\nu_\mu$ charged current interactions in our standard detector in a standard year. The result is given in Table 4.

Another obviously interesting quantity is the number of high momentum transfer $\mu \to \mu$ scattering events in our standard detector. We call an event "interesting" if it occurs

*) The quoted ratio of ν to $\bar\nu$ cross-sections is somewhat smaller than the one measured at present energies. To obtain it, we have used the Q^2-dependent structure functions of Duke and Owens[7]) and we have set $E_\nu \sim$ 0.5-1 TeV.

Table 3

Number of neutrino interactions in a "standard detector" (defined in text) per 10^7 seconds of running with $\mathcal{L} = 10^{33}$ cm^{-2} s^{-1}

		ν_e from D (= ν_μ from D)	$\bar{\nu}_e$ from $\bar{D}$ (= ν_μ from $\bar{D}$)	ν_e from F^+ (= ν_μ from F^+)	$\bar{\nu}_e$ from F^- (= $\bar{\nu}_\mu$ from F^-)	ν_e from Λ_c (= ν_μ from Λ_c)	ν_τ from $F^- \to \tau^- \to \nu_\tau$ plus $F^+ \to \nu_\tau$	$\bar{\nu}_\tau$ from $F^- \to \tau^+ \to \bar{\nu}_\tau$ plus $F^- \to \bar{\nu}_\tau$	Total neutrino interactions
LHC	opt.	8.4×10^4	4.6×10^4	6.3×10^4	3.5×10^4	6.7×10^4	1.1×10^4	3.9×10^3	6.2×10^5
	pess.	8.9×10^4	4.9×10^4	3.3×10^4	1.8×10^4	3.7×10^4	2.9×10^3	1.0×10^3	4.6×10^5
SSC	opt.	2.5×10^5	1.4×10^5	1.9×10^5	1.1×10^5	2.0×10^5	3.3×10^4	1.2×10^4	1.9×10^6
	pess.	2.7×10^5	1.5×10^5	1.0×10^5	5.6×10^4	1.1×10^5	8.8×10^3	3.1×10^3	1.4×10^6

Table 4

Number of charged-current muon-induced interactions in the same conditions as in Table 3

		$\mu^+ \to \bar{\nu}_\mu$ from D	$\mu^- \to \nu_\mu$ from $\bar{D}$	$\mu^+ \to \bar{\nu}_\mu$ from F^+	$\mu^- \to \nu_\mu$ from F^-	$\mu^+ \to \bar{\nu}_\mu$ from Λ_c	Total CC μ-interactions
LHC	opt.	2.8×10^4	5.2×10^4	2.1×10^4	3.9×10^4	2.2×10^4	1.6×10^5
	pess.	3.2×10^4	5.8×10^4	1.2×10^4	2.2×10^4	1.3×10^4	1.4×10^5
SSC	opt.	8.6×10^4	1.6×10^5	6.5×10^4	1.2×10^5	6.9×10^4	5.0×10^5
	pess.	9.3×10^4	1.7×10^5	3.5×10^4	6.5×10^4	3.8×10^4	4.0×10^5

with a momentum transfer $Q^2 > Q_0^2 \sim 100$ GeV^2: the approximate upper limit for which good data already exist. The total cross-section of interesting events for incident energy E_μ is, in the conventional notation, and upon neglect of weak effects:

$$\sigma(E_\mu)\Big|_{Q^2>Q_0^2} = 2\pi\alpha^2 \int_{Q_0^2}^{2m_p E_\mu} \frac{dQ^2}{Q^4} \int_{Q_0^2/2m_p E_\mu}^{1} dx \, \frac{F_2(x)}{x} \left(1+(1-y)^2\right)$$

$$\sim \frac{8}{3}\pi\alpha^2 F_2(0) \frac{1}{Q_0^2} \ln \frac{2m_p E_\mu}{Q_0^2} \qquad (14)$$

$$\sim \left(2\cdot 10^{-33}\ \text{cm}^2\right)\left(\frac{100\ \text{GeV}^2}{Q_0^2}\right) \ln \frac{2m_p E_\mu}{Q_0^2} \ln^{-1} \frac{2m_p (1\text{TeV})}{100\ \text{GeV}^2}$$

In the above estimate, we have used $F_2^{\mu\mathcal{N}}(0) \sim 0.4$ [with $\mathcal{N} = (p+n)/2$] and the fact that $(1-y)^2$ approximately averages to 1/3. The number of interesting muon events in our standard detector in a "year" of $Y = 10^7$ s is given in Table 5. Clearly, the rates of Table 5 are fairly large. For a dedicated muon experiment, a target much smaller than our "standard" ($\rho = 5$ gr/cm^3, $L = 25$ m) neutrino detector may well suffice.

Table 5

Number of "interesting" ($Q^2 > 100$ GeV^2) events for conventional electromagnetic muon scattering in the same conditions as in Tables 3 and 4

		$\mu^+ \to \mu^-$ from D ($= \mu^- \to \mu^-$ from $\bar{D}$)	$\mu^+ \to \mu^+$ from F^+ ($= \mu^- \to \mu^-$ from F^-)	$\mu^+ \to \mu^+$ from Λ_c	μ^+	Total μ^-	$\mu^+ + \mu^-$
LHC	opt.	2.1×10^7	1.6×10^7	1.3×10^7	5.1×10^7	3.8×10^7	8.9×10^7
	pess.	2.6×10^7	9.6×10^6	7.9×10^6	4.4×10^7	3.6×10^7	8.0×10^7
SSC	opt.	3.5×10^7	2.6×10^7	2.0×10^7	8.1×10^7	6.1×10^7	1.4×10^8
	pess.	4.4×10^7	1.6×10^7	1.3×10^7	7.3×10^7	6.0×10^7	1.3×10^8

All of the above considerations refer to pp machines with $\mathcal{L} = 10^{33}$ cm^{-2} s^{-1}. A $\bar{p}p$ option is likely to have a two orders of magnitude smaller luminosity; all of our estimated event rates would accordingly decrease by a factor ~ 100. The prompt "free" lepton beams are a good physics reason to aim at the pp option for a collider.

III. COMPARISON OF THE "FREE" ν-BEAMS WITH BEAM-DUMP GENERATED ONES

It is interesting to compare the properties of our "free" neutrino beams with the neutrino beam that could be generated in the beam dump with which the same collider facility is necessarily equipped[8]. Let d be the number of times per day that the collider's beams are dumped, before proceeding to a new refilling. Let N_p ($N_{\bar{p}}$) be the number of protons (antiprotons) dumped each time. Let N_B be the number of bunches of the collider. We shall normalize our forthcoming considerations to the parameters[2] listed in Table 6. The extracted

Table 6

Educated guesses of some parameters of future colliders

		d	N_p	$N_{\bar{p}}$	N_B
LHC	(pp)	3	2.5×10^{13}		3564
	($\bar{p}p$)	3	2.5×10^{13}	5×10^{11}	108
SSC	(pp)	3	7×10^{13}		6000

p's ($\bar{p}$'s) must be blown up before hitting the dump. If the cone that the blown-up beams form has an aperture of $\sim$ 1 mrad or less, the neutrinos from the dump are sufficiently well collimated to do experiments with. The c.m.s. energy in the collisions of the extracted particles with the nucleons in the dump is $\sqrt{s} \sim 122$ (194) GeV at the LHC (SSC). The laboratory energy distribution of the produced charmed particles (and prompt lepton beams) is the same as that of the particles produced at the pp ($p\bar{p}$) collision points. (This is Feynman-x scaling, broken only by scaling violations in the fragmentation functions, presumably not very important for diffractively produced particles). What should be very different at lower c.m.s. energy is the charm multiplicity σ_c/σ_{tot}. We shall estimate in Appendix A σ_c/σ_{tot} to be of order 2.3% (3.4%) at $\sqrt{s} \simeq 122$ (194) GeV. Given the approximate equality in shape of the beam-beam and beam-dump generated neutrino fluxes, the simplest way to compare the two beams is to compare the normalization of the fluxes, without reference to a particular detector.

The number of leptons of type ℓ produced by all of the dumped N_p protons is

$$N_\ell \sim N_p \frac{\sigma_c}{\sigma_{tot}} \sum_{\mathbb{C}} \frac{\sigma(\mathbb{C})}{\sigma_c} BR(\mathbb{C} \to \ell) \equiv N_p \frac{\sigma_c}{\sigma_{tot}} \langle BR(\mathbb{C} \to \ell) \rangle \tag{15}$$

where we have counted only the most energetic leptons, produced in the decay of the charmed particles created in the "first generation" proton interactions in the dump. The time-averaged ratio of the beam-dump flux to the beam-beam flux of Eq. (11) is given by

$$\frac{\Phi_\ell(\text{beam dump})}{\Phi_\ell(\text{beam-beam})} = \frac{365\, d}{\pi\, 10^7 \text{ secs}} N_p \frac{\sigma_c}{\sigma_{tot}}\bigg|_{bd} \left(\frac{\mathcal{L}}{2} \sigma_{tot} \frac{\sigma_c}{\sigma_{tot}}\bigg|_{bb} \right)^{-1} \tag{16}$$

Substituting the parameters of Table 6 and the quoted cross-section ratios, we obtain

$$\frac{\Phi_\ell(bd)}{\Phi_\ell(bb)} = 2.8 \left(\frac{d}{3}\right)\left(\frac{N_p}{2.5 \cdot 10^{13}}\right)\left(\frac{10^{33}\, cm^{-2} s^{-1}}{\mathcal{L}}\right) \quad (LHC) \tag{17a}$$

$$= 9.6 \left(\frac{d}{3}\right)\left(\frac{N_p}{7 \cdot 10^{13}}\right)\left(\frac{10^{33}\, cm^{-2} s^{-1}}{\mathcal{L}}\right) \quad (SSC) \tag{17b}$$

This means that, on average, the beam-dump ν-beam is $\sim$ 3(10) times more intense than the beam-beam ν-beam in the pp versions of the LHC (SSC). In the $\bar{p}p$ version of the LHC this intensity ratio would increase to $\sim$ 0(300): The beam-beam generated beams are in this case of rather low intensity. The transverse size of the beam-dump generated ν-beam at a detector is bound to be bigger that what could be achieved with a beam-beam generated beam. For a sufficiently wide detector, the number of ν interactions per year can be estimated by multiplying the numbers in Table 3 by the corresponding flux ratios of Eq. (17). The result of this exercise for the total number of neutrino interactions per year in our standard (ρ = 5 gr/cm, L = 25 m) detector is 1.7×10^6 (1.2×10^6) at the LHC in our optimistic (pessimistic) model. With our assumption $N_p(\bar{p}p) = N_p(pp)$, these numbers apply to the $\bar{p}p$ version of LHC as well. At the SSC, the number of interactions is an order of magnitude larger, to wit 1.8×10^7 (1.3×10^7). It would clearly be nice to be able to afford this more expensive version of neutrino beams. An interesting remark concerns the number of neutrino interactions per extracted bunch in our standard detector. To obtain it, divide the number of interactions per year by $365/\pi$ (days in a physicist's year), by 3 (the assumed value of d: dumps a day) and by N_B, specified in Table 6. The results are of the order of 1, 36 and 7 for the pp, $\bar{p}p$ versions of the LHC, and for the SSC, respectively. In the last two cases we may have been comtemplating too large (!) a neutrino detector, unless one can extract the beam by fractions of a bunch.

The beam-dump generated beams have, in spite of their favorable intensity, several short-comings that we now discuss. A first, easily solvable problem of the beam-dump generated beams is the following. The decay length of a charmed particle at the relevant energies is of order 12 cm (30 cm) at the LHC (SSC), see Eq. (1). This is larger than an interaction length ℓ_i in a solid target of density ρ:

$$\ell_i = \left(\sigma_{c\nu}\, \rho\, N_A\right)^{-1} = 7\,\text{cm}\left(\frac{30\,\text{mb}}{\sigma_{c\nu}}\right)\left(\frac{8\,\text{gr cm}^{-3}}{\rho}\right) \tag{18}$$

Thus, the first few interaction lengths of dump ought to be made of thin, well separated slabs, to let the charmed particles decay.

A second (unsolvable?) problem concerns the number of hard muons N_μ produced per extracted bunch:

$$N_\mu = \frac{N_p}{N_B}\,\frac{\sigma_c}{\sigma_{tot}}\,\langle BR(c\to\mu)\rangle \sim \begin{cases} 1.6\cdot 10^7 & (\text{LHC, pp}) \\ 5.3\cdot 10^8 & (\text{LHC, p's from } \bar{p}p) \\ 4.0\cdot 10^7 & (\text{SSC, pp}) \end{cases} \tag{19}$$

These numbers are so enormous that a costly muon shielding (or several kilometers of soil) are certainly necessary downstream of any ν-detector. In addition, many slow muons are generated by the decay of "slow" secondary pions in the dump's interslab spaces. Detailed physics with these abrupt spills of muons is certainly out of the question. A possible solution may be to "dump" the beam on an internal gas-jet target.

Another interesting question is the comparison between the necessary beam dump that we have just discussed and a hypothetical "dedicated" beam dump experiment. Let the collider be operated as a dedicated proton accelerator for N_h hours/day, and let these protons be dumped in the dump. Assume the collider to accelerate protons in this mode at a rate of $N_p^D = 10^{14}$ p/minute, where "D" stands for "dedicated to dumping". The ratio of dedicated (D) to necessary (N) neutrino fluxes from the dump is

$$\frac{\Phi_\nu^D}{\Phi_\nu^N} = \frac{3}{d} N_h \left(\frac{N_p^D}{10^{14}\ p's\ min^{-1}}\right) \begin{cases} 80\ (2.5\cdot 10^{13}/N_p) & LHC \\ 30\ (7\cdot 10^{13}/N_p) & SSC \end{cases} \qquad (20)$$

For our standard choices of parameters, a one hour a day dedicated running produces 80(30) times more neutrino events at the LHC (SSC) than the necessary beam dump. The total numbers of neutrino events per standard year per standard detector for $N_h = 1$ (and our other "standard" choices of parameters) is summarized in the following table. Clearly the dedicated

Table 7

Comparison of the numbers of neutrino events (per standard year and detector) in various scenarios

		Beam-beam	Necessary beam dump	Dedicated beam dump
LHC (pp)	opt.	6.2×10^5	1.7×10^6	1.4×10^8
	pess.	4.6×10^5	1.3×10^6	1.0×10^8
SSC	opt.	1.9×10^6	1.8×10^7	5.4×10^8
	pess.	1.4×10^6	1.3×10^7	3.9×10^8

beam dump is the best (though most expensive) option for neutrino physics, while the beam-beam generated muons are the only useful ones for physics (unless an extremely slow extraction of protons is feasible).

IV. COMPARISON OF THE COLLIDER'S MUON BEAM WITH OTHER FACILITIES

The very intense prompt muon beam from a collider can be used for the study of μ-nucleon scattering at large Q^2, as indicated in Table 5, that refers to total number of events with $Q^2 > 100$ GeV^2. Since Q^2 is a measure of the "depth" to which the interacting particles are analyzed, it is also interesting to compare different facilities in terms of expected cross-sections and number of events in various ranges of Q^2. The results of such a comparison are summarized in Fig. 2, which we proceed to explain.

In Fig. 2a we compare the cross-sections for $e^+p \to e^+X$ and $\mu^+\mathcal{N} \to \mu^+X$ scattering in bins of Q^2 [$\mathcal{N} = (p+n)/2$]. The (ep) results refer to the parameters of the HERA machine and those of a hypothetical ep collider in the LEP tunnel ($E_e = 100$ GeV, $E_p = 8$ TeV). The cross-sections for the ($\mu^+\mathcal{N}$) results are averaged over the "pessimistic" prompt muon fluxes that we have computed for the LHC and SSC machines in Appendix B. All calculations include the

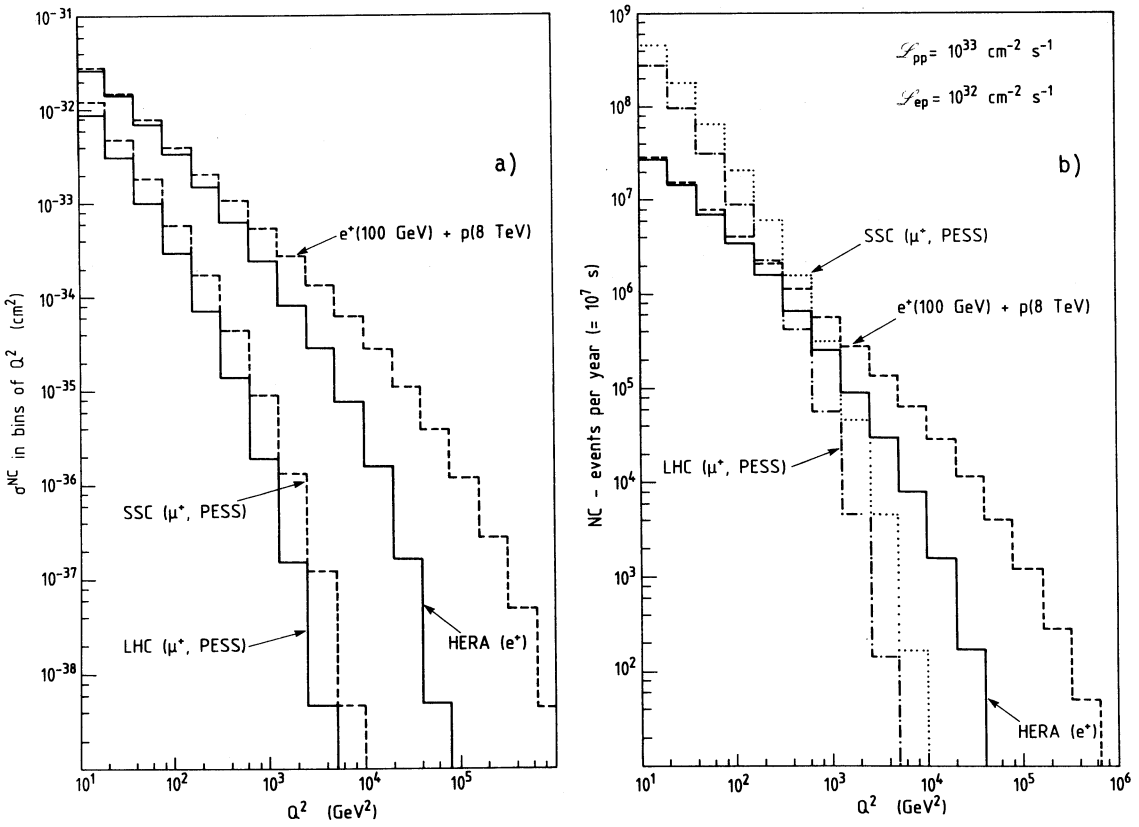

Fig. 2 Unpolarized neutral current cross-sections and event rates at various facilities.

weak and electromagnetic effects of the standard SU(2) × U(1) model and employ the Q^2-dependent structure functions of Duke and Owens[7]. The cross-sections for ep colliders extend to higher values of Q^2 than those of the "secondary" $\mu\mathcal{N}$ collisions since the center of mass energy of the former is higher. This effect is partially compensated by the fact that the "effective luminosity" of the $\mu\mathcal{N}$ collisions on a sufficiently long target is very high. This is shown in Fig. 2b, where we compare number of events in Q^2-bins for a standard year of running (10^7 secs). The ep event rates are obtained with a luminosity of 10^{32} cm^{-2} s^{-1}, whereas the $\mu\mathcal{N}$ results correspond to a pp luminosity of 10^{33} cm^{-2} s^{-1} and our "standard" target ($\rho = 5$ gr/cm^3, L = 25 m). We have not reduced the muon flux by the effect of the hadron shield, which may diminish the rates by a factor of two. The conclusions from Fig. 2b are clear. The dedicated ep colliders are superior in terms of possible statistics at the highest values of Q^2, the most interesting domain for possible "new physics". But the high statistics of $\mu\mathcal{N}$ scattering at lower Q^2 may permit the search for very rare events. Also, nuclei are unlike protons, muons may be different from electrons, and fixed target experiments are definitely complementary to the ones at a collider.

V. SUMMARY AND CONCLUSIONS

We have argued that the "free" prompt muon and neutrino beams from future pp colliders are sufficiently intense, energetic and collimated to be of interest to physics. We believe

that their potential ought to be considered when choosing the characteristics of these machines. The most obvious example is the choice between pp and $\bar{p}p$ options: we vote for pp.

The physics that can be explored with the prompt muon beam from a pp collider compares favorably with that of approved or hypothetical ep colliders, at all but the highest values of $Q^2 > 1000$ GeV^2, as can be seen in Fig. 2b.

The "free" neutrino beams are energetic and intense enough to deserve utilization, but the more expensive beams from beam dumps equipped with muon shielding are considerably more intense, as can be seen in Table 7.

APPENDIX A

CHARM PRODUCTION CROSS-SECTIONS

Our estimates of prompt lepton fluxes depend linearly on the total cross-section σ_c for charm production in pp ($\bar{p}p$) collisions at $\sqrt{s}$ = 0.1 to 40 TeV. Unfortunately, both the experimental and the theoretical scenario on charm production even at the energies available in today's accelerators are fairly confusing. The situation (as of July 1983) is summarized[9] in Fig. 3. The data are spread over more than an order of magnitude and are sometimes inconsistent. The theoretical models[10], though allegedly inspired in the same theory (QCD), show a similar or even larger spread. A glance at Fig. 3 suffices to imagine what the spread of the theoretical predictions would be, if they were to be extrapolated two or three orders of magnitude up in energy, to the regime of interest to us. We are faced with an interesting situation in which we can neither trust theory nor heavily rely on experiment. Our naive way out is explained in this Appendix.

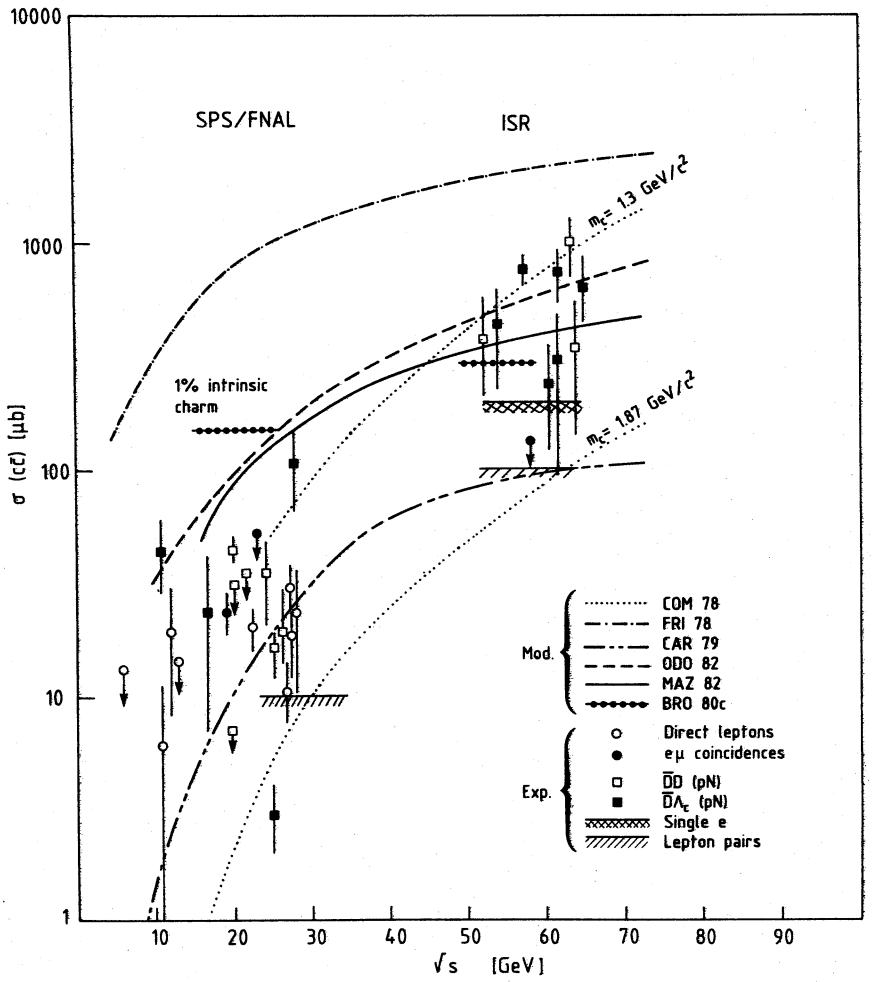

Fig. 3 Summary of experiments and models of charm production in pp collisions (from ref. 9).

In Fig. 4 we have summarized some data for the multiplicities $\langle n_i \rangle = \sigma(pp \to i)/\sigma_{tot}$ of different particles $i = \pi, K, D, \bar{p}, \Lambda_c$ in pp collisions[11], $n_i = \sigma(pp \to i)/\sigma_{tot}$. The few data points on charm multiplicities that are shown are either directly measured in pp collisions, as for the ISR data, or extracted from measurements in nuclear targets with an assumed $A^{2/3}$ dependence (as advocated by Halzen[5] whose "data" we have borrowed). The trend of multiplicities as a function of energy $\langle n_i(s) \rangle$ for particles of different masses follow curves that are not dissimilar. To make this statement more precise, we have drawn Figs. 5 and 6. Fig. 5a shows fits of the form[11] $\langle n_i(s) \rangle = a_i + b_i \ln s + c_i s^{\frac{1}{2}}$, for $i = \pi^{\pm}, K^{\pm}, \bar{p}$. The most naïve expectation based on dimensional analysis would be that the production cross-section for a particle of mass m_i is proportional to m_i^{-2}. That this is approximately correct at high energy becomes apparent in Fig. 5b, where we have plotted $m_i^2 \langle n_i(s) \rangle$. Obviously this expectation cannot be correct close to the different production thresholds s_{TH}^i. Moreover, $m_i^2 \sigma(pp \to i)$ is dimensionless, and may be expected to be a function of a dimensionless variable.

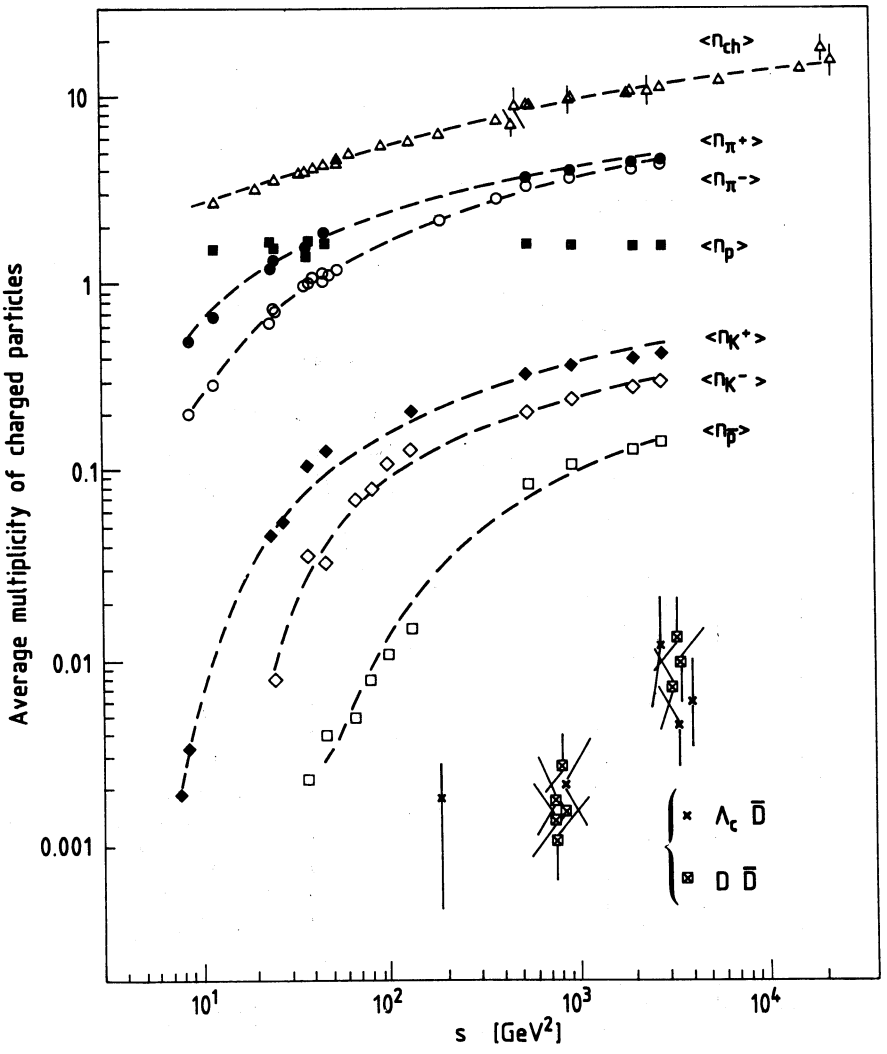

Fig. 4 Particle multiplicities as a function of energy in pp collisions ($\pi, K, p, \bar{p}$ and ch from ref. 11).

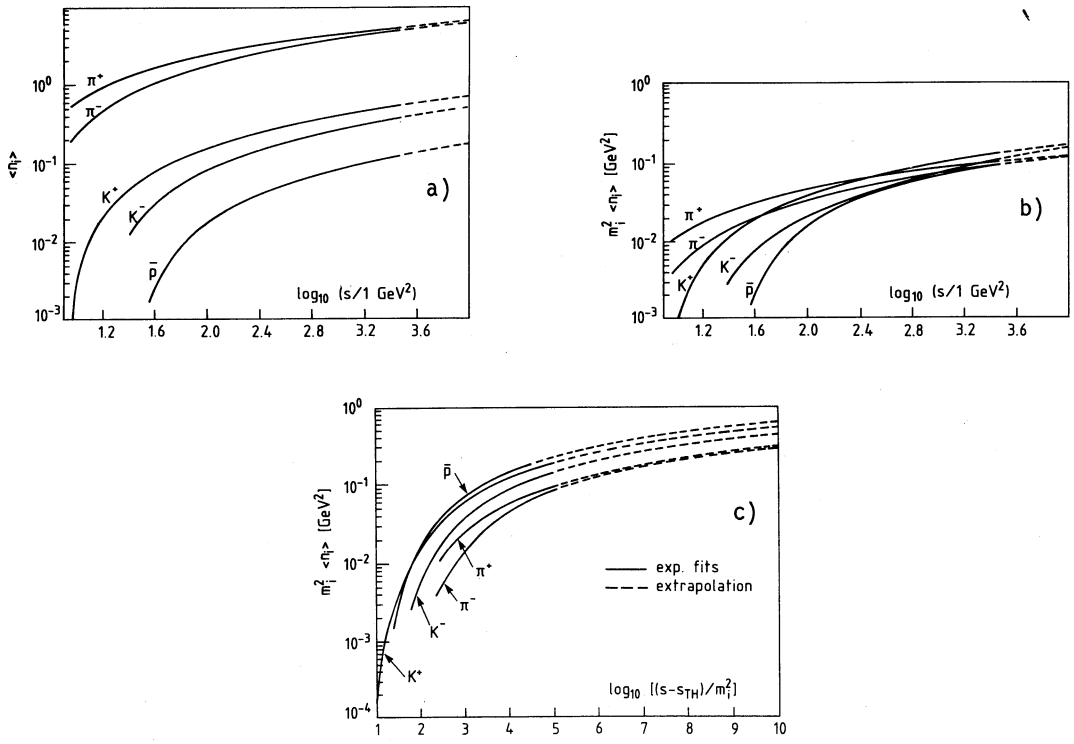

Fig. 5 a) Fits to some of the particle multiplicities of Fig. 4. b) Multiplicities times the square of the produced particle's mass. c) Same as (b), plotted as a function of the variable defined in Eq. (A1).

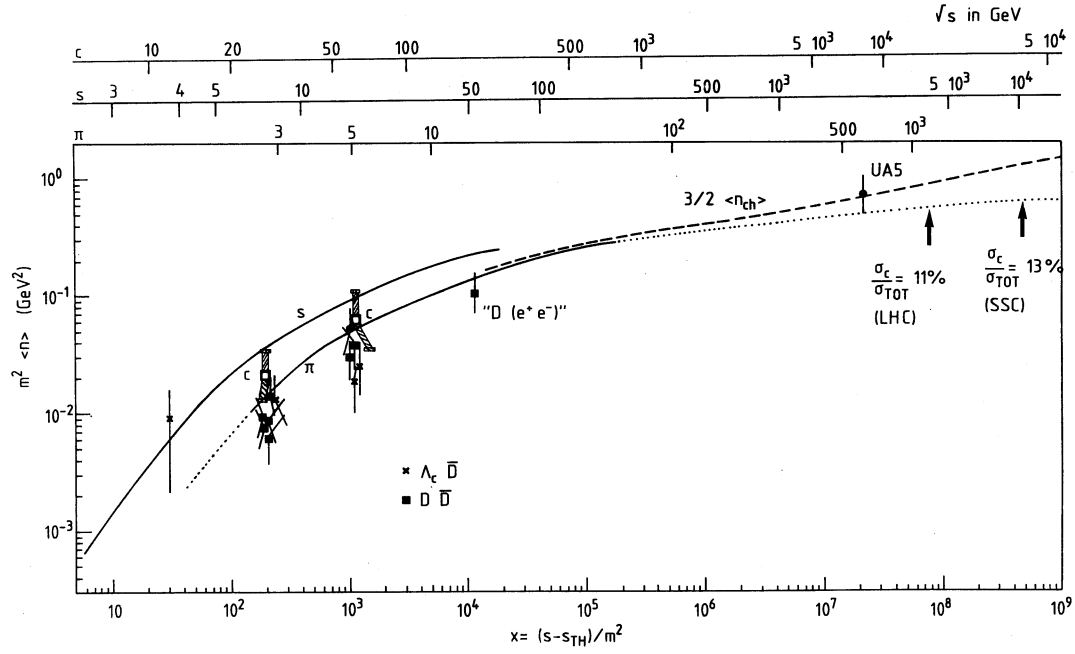

Fig. 6 Comparison of pion, strange particle and charm multiplicities in pp collisions in terms of the approximate scaling law of Eqs. (A1).

In Fig. 5c we "cure" these problems[9] by plotting $m_i^2 \langle n_i \rangle$ as a function of $x = (s - s_{TH}^i)/m_i^2$. The multiplicities $\langle n_i \rangle$ that in Fig. 5a were displaced by orders of magnitude in the vertical and/or horizontal directions have now considerably coalesced, and show a striking similarity in their shape. We have "detected" a rough universal scaling law for the production cross-sections in pp collisions of particles of different masses*)

$$m_i^2 \sigma_i(pp \to i) \sim f(x)$$
$$x = x_i \equiv (s - s_{TH}^i)/m_i^2 \qquad \text{(A1)}$$

where f(x) is a particle-independent universal function, normalized by construction to vanish at threshold: f(0) = 0. Clearly, this scaling law could not be expected to be better than it is: we compare particles with specific charges, neglect all reference to resonances, spin, isospin, etc. But the scaling law[13], when extended to charm production in the next paragraph, is presumably better (it is at least more predictive) than what is shown in Fig. 3.

In Fig. 6 we apply the previous considerations to "total" cross-sections for pion production, strange particle and charmed particle production. The curve labelled "π" is $(3/2)m_\pi^2[\langle n(\pi^+)\rangle + \langle n(\pi^-)\rangle]$, we have estimated the π^0 multiplicity to be the average of π^+ and π^- multiplicities. The curve labelled "S" is $(3/2)m_K^2\langle n(K^+)\rangle$, an estimate of the total strange particle production multiplicity, multiplied by m_K^2. The estimate is based on a simple counting of the three-body (i.e. $pp \to p\Lambda K^+$) and four-body channels (i.e. $pp \to ppK^+K^-$) that are dominant at relatively low energy. The points for $\Lambda_c\bar{D}$ and $\bar{D}D$ production are those of Fig. 4, multiplied by m_D^2 and plotted in terms of the corresponding x (see Eq. A1). The points labelled "C" are underestimates of total charm cross-sections: the sum of the averages of the $\bar{\Lambda}_c D$ and $\bar{D}D$ points in the same Figure (we have neglected F production, that in our naïve world would be $\sim \frac{1}{2}$ of D production: there are two types of F's and four types of D's, and $m_F \sim m_D$). The point labelled $D(e^+e^-)$ is a guess[5] based on the measured D multiplicity in e^+e^- annihilation well above threshold, and transferred to a pp energy scale by assuming $s_{eff}(pp) \sim \langle x^2 \rangle s(e^+e^-)$. The dashed line labelled $(3/2)\langle n_{ch}\rangle$ is an estimate of the pion multiplicity at very high energy, and corresponds to a fit containing a $(\log)^2$ term. The dotted line is an extrapolation of the lower energy fit to the pion multiplicity, whose dominant term at high energy is a simple logarithm. A recent measurement of $3\langle n_{ch}\rangle/2$ by the UA5 collaboration is also shown. In estimating charm production at future colliders we shall conservatively use the dotted line. It corresponds to values of σ_c/σ_{tot} of 11% and 13% at the LHC and SSC collider energies, respectively. The values of σ_c/σ_{tot} at the same machine's beam-dump fixed target energies are 2.3 and 3.4%. Notice that our extrapolation in energy of the charm production cross-section is a very long shot. But in the sense of our scaling law in terms of $x \sim s/m_i^2$, the extrapolation from the UA5 point (for which $m_i \simeq m_\pi$) to the x-values relevant to charm production at future colliders, is much more modest.

We conclude that a 10% charm production "efficiency" at future colliders is a conservative estimate, that is unlikely to be wrong by more than a factor of 2 to 4, either way.

---

*) Here we shall not dwell on possible improvements[12] of these naïve expressions (e.g. the substitution of m_i by the transverse mass in the definition of x) nor on the comparison of $m_i^2\langle n_i\rangle$ for different reactions ($pp, \pi p, \gamma p, \nu p$ ...).

APPENDIX B

NEUTRINO AND MUON FLUXES

In this Appendix we give more detailed results for the prompt lepton fluxes as a function of energy and angle. The corresponding average energies are used in Chapter II to estimate the number of events per year in a standard detector.

Let $c(x)$, with $x = E_c/E_p$, by the Feynman-x distribution of a given charmed particle in $pp(\bar{p}p)$ collisions. We adopt normalized distributions of the form:

$$c(x) = (1-x)^n / (n+1) \tag{B1}$$

Let $L(y)$, with $y = E_\ell/E_c$, be the longitudinal momentum distribution (in an "infinite" momentum frame) of a given lepton ℓ in the decay $c \to \ell + X$ ($\ell = \nu_\mu, \nu_e, \mu$). For a "three-body" fundamental decay such as $c \to \mu^+ \nu_\mu s$ and in the approximation $m_s^2/m_c^2 \ll 1$ the normalized shape of $L(y)$ is

$$L(y) = \begin{cases} 2 - 6y^2 + 4y^3 & \text{for } \ell = \mu, e \quad \text{(B2a)} \\ \frac{5}{3} - 3y^2 + \frac{4}{3}y^3 & \text{for } \ell = \nu_\mu, \nu_e \quad \text{(B2b)} \end{cases}$$

We do not give here the exact expressions for $m_s \neq 0$, which are more cumbersome. Let $z_\ell = E_\ell/E_p$ be the longitudinal momentum fraction of the lepton in the chain $pp \to X' + c(c \to \ell + X)$. The normalized flux of the lepton beam is then

$$\frac{dN}{dz_\ell} = \int_0^1 c(x)\, L(y)\, \delta(z_\ell - xy)\, dx\, dy \tag{B3}$$

for which it is easy to obtain explicit analytical expressions. A good approximation of the effects of $m_s \neq 0$ is to introduce the quantity $\beta = m_c^2/(m_c^2 - m_s^2)$ and make the following corrections to Eq. (B2)

$$L(y) = \begin{cases} 2\beta - 6\beta^3 y^2 + 4\beta^4 y^3 & \text{for } \ell = \mu, e \quad \text{(B2c)} \\ \frac{5}{3}\beta - 3\beta^3 y^2 + \frac{4}{3}\beta^4 y^3 & \text{for } \ell = \nu_\mu, \nu_e \quad \text{(B2d)} \end{cases}$$

We compute the normalized total fluxes of a given lepton type by summing the individual fluxes we just described (that correspond to a particular charmed particle D, F, Λ_c) with the assumed

relative weights of particle production given in Table 1. We have checked the above analytical results against a Monte Carlo calculation (with m_c = 2 GeV, m_s = 0.5 GeV) that proceeds along similar lines, and which we shall heavily rely upon for the computation of the angular spread of the beams.

Figure 7 exhibits our results. The neutrino fluxes are presented as $z_\nu dN/dz_\nu$ or $E_\nu dN/dE_\nu$, which is a measure of the distribution of events as a function of energy. The muon fluxes are shown as dN/dz_μ. The calculation of the ν_τ fluxes proceeds along similar lines and involves an extra convolution (or Monte Carlo step) in the case of the "fast secondary" ν_τ's, $F^- \to \bar{\nu}_\tau \tau(\tau \to \nu_\tau X)$. We do not give the (rather obvious) details of this calculation. It is clear from Fig. 7 that the lepton fluxes are still considerable at energies that are a good fraction, say 40%, of the machine energy E_p.

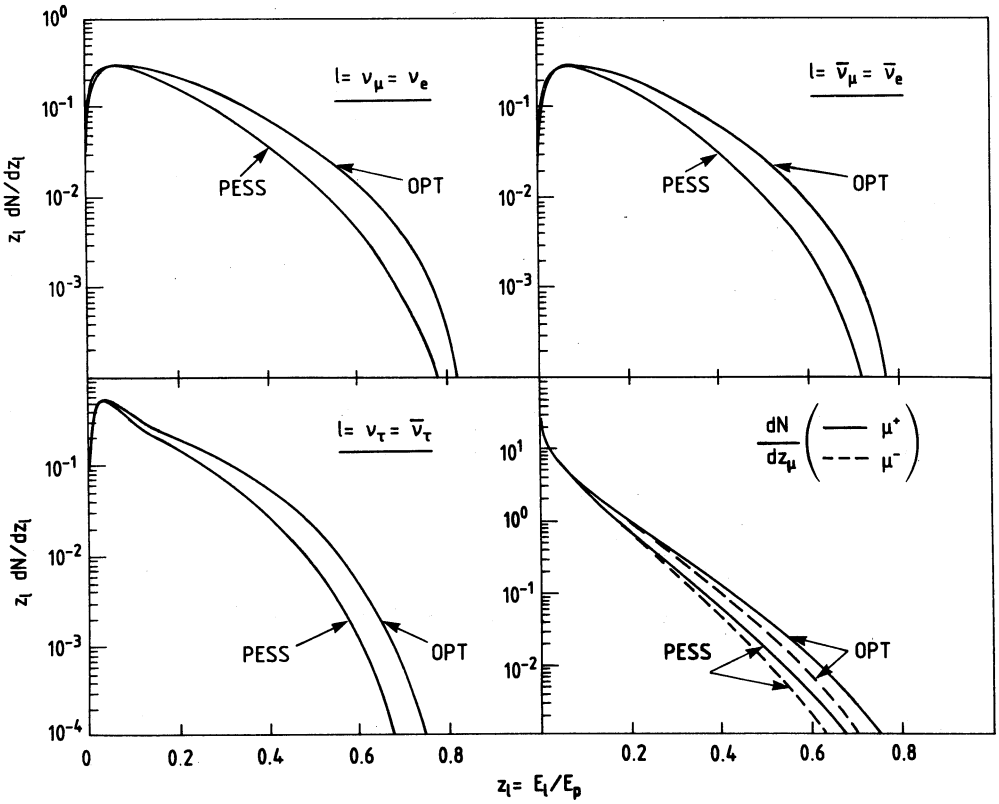

Fig. 7 Neutrino and muon fluxes as a function of z = E(lepton)/E(proton).

In Fig. 8 we give Monte Carlo results for the angular spread of the lepton beams, as a function of the angle θ between the lepton momentum and the proton beam direction. For neutrinos we show $E_\nu(\theta_\nu)dN/d\cos\theta_\nu$ which represents the event distribution at a detector, as a function of angle, while for muons we give $dN/d\cos\theta_\mu$, a measure of the number of muons in the beam as a function of angle. We investigate various assumptions on the x-distribution of the parent charmed particles and use a Gaussian p_T distribution with $\langle p_T \rangle$ = 1 GeV. Even if $\langle p_T \rangle$ were to be doubled, the beam divergence is of order 1 mrad. At 100 meters from a collision point these beams could be intercepted by a target of very modest transverse dimensions.

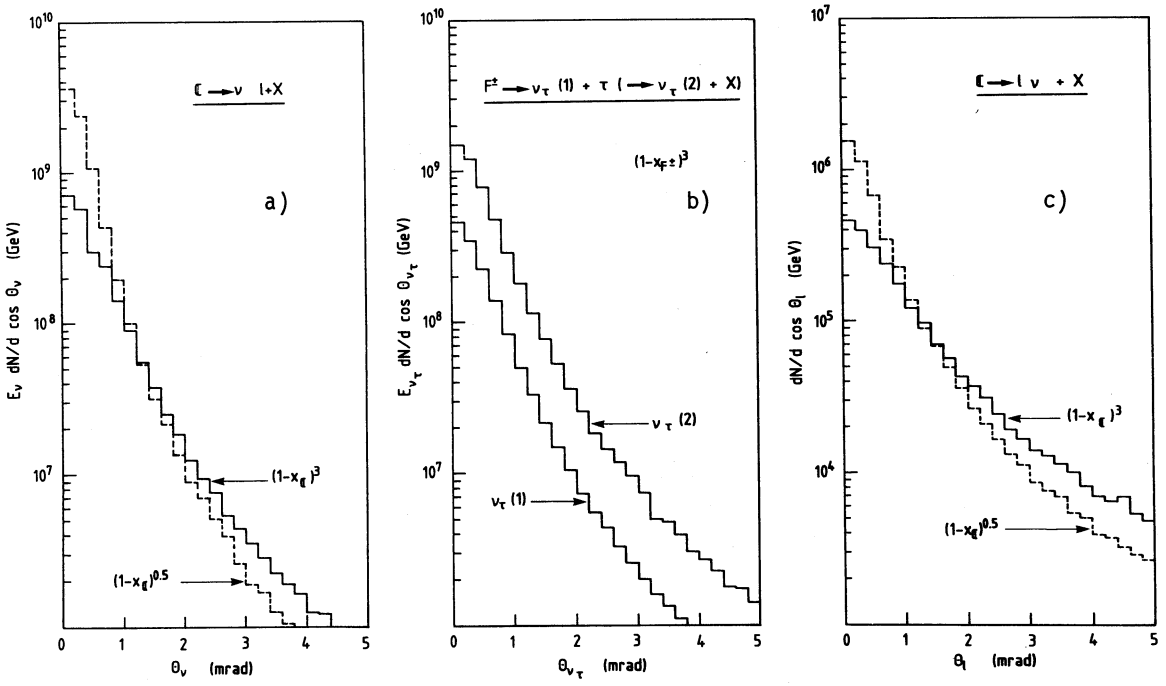

Fig. 8 Angular shapes of neutrino and muon fluxes corresponding to $\langle p_T \rangle$ = 1 GeV.

The shape of the muon beam given in Fig. 7 refers to muons as they come from a collider's interaction point. But the muons are degraded in energy and intensity as they cross the hadron shield, or a certain amount of soil. We have estimated these effects, but not the additional angular spread induced by muon interactions prior to a detector. A fair approximation to the energy loss of a muon in a material of density ρ and atomic number of weight (Z,A) is given by[14]

$$-\frac{dE}{dx} = \mathcal{R}(1+bE_\mu) = \frac{2Z}{A}\left(\frac{\rho}{\rho(H_2O)}\right)\left[2.12\ \frac{MeV}{cm}\right]\left(1+\frac{Z E_\mu}{8\,TeV}\right) \qquad \text{(B4)}$$

Muons with TeV energies are more than minimum ionizing, due to the effects of bremsstrahlung, pair creation and nuclear interactions. Eq. (B4) is an approximation to what is theoretically and experimentally known about these effects. Let E_L be the energy of a muon that has travelled a distance L through a certain material. On the average the original energy E_0 of that muon is, according to Eq. (B4)

$$E_0(E_L) = \frac{1}{b}\left[(1+bE_L)\,\mathcal{R}^{bRL} - 1\right] \qquad \text{(B5)}$$

Let $dN_0/dE_0 \equiv \phi(E_0)$ be the original muon flux. The muon flux after an L-meter voyage through a dense medium is

$$\frac{dN_L}{dE_L} = \Phi_0\left(E_0(E_L)\right)\Theta(E_L) \qquad \text{(B6)}$$

In Fig. 9 we show the percentage of produced muons

$$\frac{N_{\mu^+}(L)}{N_{\mu^+}(0)} = \int_0^{E_L^{max}} dE_L \frac{dN_L}{dE_L} \Big/ \int_0^{E_0^{max}} dE_0 \frac{dN_0}{dE_0} \tag{B7}$$

that survive after a voyage of L kilometers in typical soil material (ρ = 2.5 gr/cm^3, Z = 10, A = 20). Since the beam is narrow and the original flux of muons is of the order of 10^6/s (for $\mathcal{L} = 10^{33}$ cm^{-2} s^{-1}), problems of radiation safety cannot simply be forgotten. Because of statistical fluctuations that we have not taken into account, the number of muons at relatively large L is underestimated in Fig. 9. Figure 10 exhibits the shape of the muon flux after different depths of soil. The results are given in terms of energy (rather than energy fractions) for the LHC and the SSC, since Eq. (B4) does not exactly "scale". Again, the high energy tails of these distributions are underestimated, as a result of the neglect of fluctuations.

In Fig. 11 we show the shape of muon fluxes after a modest number of meters of iron, a possible material for a hadron shield. For L $\lesssim$ 100 meters, the extra angular spread of the beam should be smaller than its natural width. This time we give results in terms of a scaling variable z_μ, rather than the actual energy for the two machines. For the "short" iron shields we are considering the breakdown of scaling implied by Eq. (B4) is negligible in the comparison of SSC and LHC energies. As can be seen from Fig. 11, the muon beam is still quite intense after a few tens of meters of iron shield.

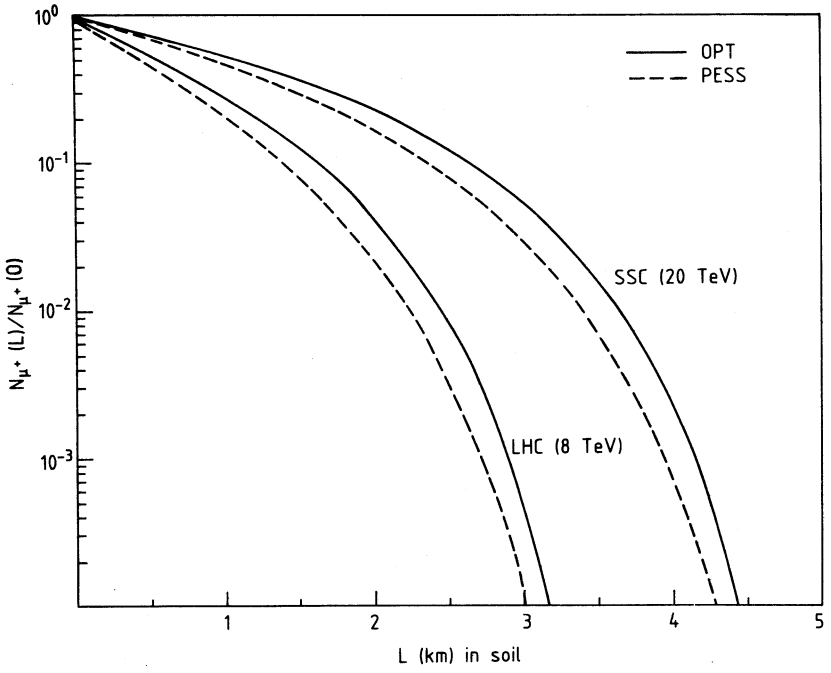

Fig. 9 Fractional number of muons as a function of depth as they travel in soil.

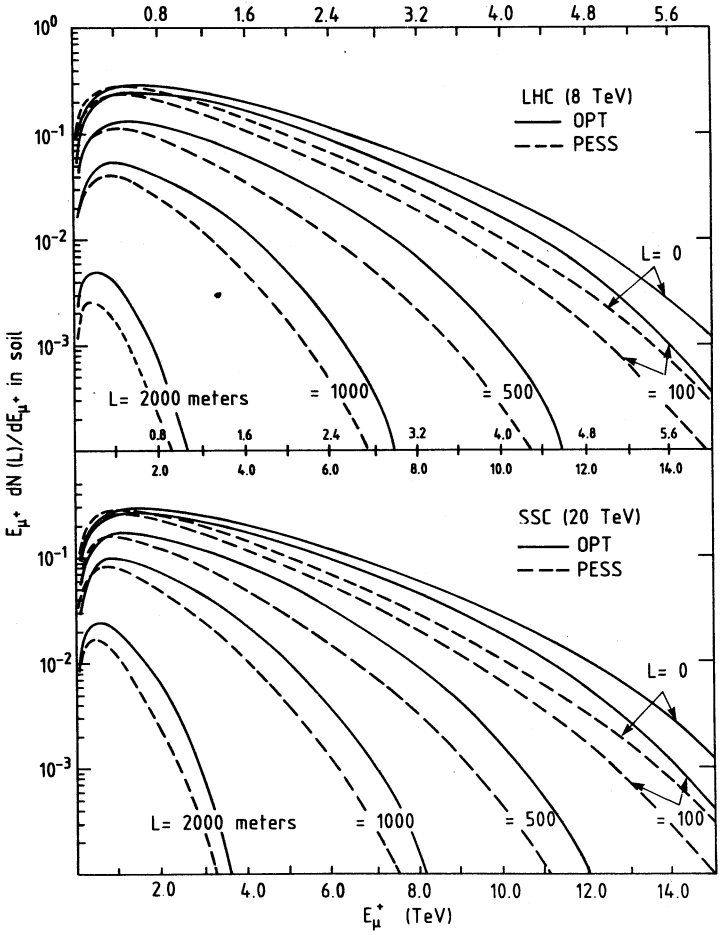

Fig. 10 Evolution of the intensity and shape of the muon flux as it travels at different depths L in soil.

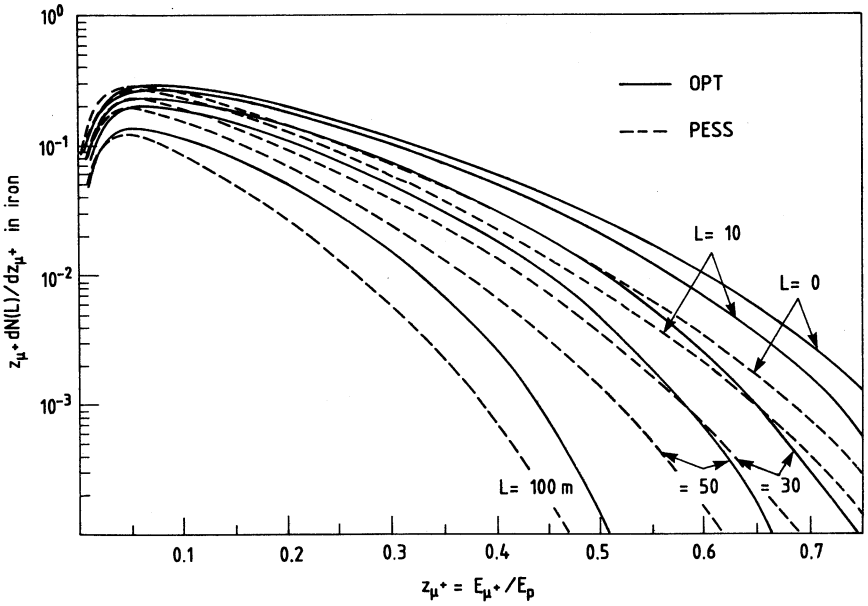

Fig. 11 Same as Fig. 10, in an iron shield.

REFERENCES

1) G. Altarelli, B. Mele and R. Rückl, Physics of ep-collisions in the TeV energy range, CERN preprint TH. 3932 (1984), see these proceedings.

2) Details on the machine design of the LHC and SSC can be found in these proceedings.

3) A. Martin *in* the Proceedings of the 21st International Conference on High-Energy Physics, Paris 1982, ed. by P. Petiau and M. Porneuf, Les Editions de Physique (Paris, 1982); R.N. Cahn, Theoretical Perspectives on Elastic and Total Cross-sections at the SSC, LBL preprint, LBL-17432 (1984).

4) M. Aguilar-Benitez et al., Phys. Lett. 123B (1983) 103.

5) For a review, see e.g. F. Halzen *in* the Proceedings of ref. 3.

6) R. Rückl, Weak decays of heavy flavours, CERN preprint (1983), to be published in Physics Reports C.

7) D.W. Duke and J.F. Owens, Q^2 dependent parametrizations of parton distribution functions, Florida State University, preprint FSV-HEP 83/115 (1984) and Erratum.

8) For a recent discussion of high energy beam-dump-generated neutrino beams, see E.L. Berger, L. Clavelli and N.R. Wright, Phys. Rev. D 27 (1983) 1080.

9) D. Drijart et al., Contribution to the High-Energy Physics Conference, Brighton (UK), 1983.

10) The theoretical models of Fig. 3 are from the following references:

COM 78 - B.L. Combridge, Nucl. Phys. B151, (1978) 429.

FRI 78 - H. Fritzsch and K.H. Streng, Phys. Lett. 78B, (1978) 447.

CAR 79 - C.E. Carlson and R. Suaya, Phys. Lett. 81B, (1979) 329.

ODO 82 - R. Odorico, Bologna preprint IFUB 82/3 (1982).

MAZ 82 - P. Mazzanti and S. Wada, Bologna Prep. IFUB 82/9 (1983).

BRO 80 - S. Brodsky et al., Phys. Lett. 93B, (1980) 251.

11) See e.g. G. Giacomelli and M. Jacob, Phys. Rep. 55 (1979) 1 and references therein. The parameters of the fits in Fig. 5 are taken from A.M. Rossi et al., Nucl. Phys. B84 (1975) 269.

12) A. De Rújula and R. Rückl, to be published.

13) A similar scaling law in terms of s/m_1^2 (see Fig. 5b) used to predict charm multiplicities from K_S multiplicities has been proposed by S. Geer et al., EP Internal Report 83-08, CERN, 1983.

14) See e.g. A. De Rújula et al., Phys. Rep. 99 (1983) 341 and references therein.